



## **NUMERICAL SIMULATION OF EARTHQUAKE – INDUCED PHENOMENA IN SAND**

**Stavros A. SAVIDIS<sup>1</sup>, Daniel AUBRAM<sup>2</sup>, Frank RACKWITZ<sup>3</sup> and Winfried SCHEPERS<sup>4</sup>**

### **SUMMARY**

The paper briefly presents the procedures converging to a realistic numerical simulation of an earthquake-induced shear wave propagation in sandy soil continua: constitutive modelling, numerical implementation and finite element simulation. The classical equivalent linear approach fails to simulate the strong non-linear material behaviour and the specific characteristics of granular soil realistically and, therefore, the incorporation of an advanced constitutive equation is needed. The elastoplastic sand model introduced herein, referred to as CSSA-Model, is based on the critical state concept as well as on the bounding surface plasticity framework and the concept of generalized plasticity. In order to capture the response of sand over a wide range of density and stress states with only one set of material parameters, the dilatancy, defined as the ratio of volumetric and deviatoric strains, enters the constitutive equation as a special function dependent on the stress and density state. After summarising requirements of the numerical implementation, simulations of element tests and seismic shear wave propagation in sandy soil layers are presented. The results show that advanced constitutive equations enable realistic predictions of excessive pore pressure development. In respect thereof, the liquefaction phenomenon merely appears as a special case for loose sand.

### **1. INTRODUCTION**

It is well known that the ground motions on soil deposits under seismic loading depend on local soil conditions, and often are larger than those of the rock outcrop. Especially granular soils may underlie a complete loss of shear resistance resulting in large permanent deformations and lateral spreading of earth structures. However, this liquefaction phenomenon under undrained conditions only occurs if the sand is sufficient loose. The same sand in a dense state would evoke cyclic mobility and limited deformation.

In the last decades great effort has been made to predict the soil response beforehand of an earthquake to minimise conditions to which buildings or infrastructure are subjected. One of the key issues is the realistic simulation of shear wave propagation, which requires an appropriate constitutive equation for the granular material to model its specific characteristics, especially under cyclic loading conditions. Due to shear loading under the same stress state, the volume of a dense sand sample dilates, whereas a loose sand contracts. Irrespective of the current void ratio, sand exhibits an isochoric response if shearing continues, which is well-known as critical state.

---

<sup>1</sup> Soil Mechanics and Foundation Engineering Division, Technical University of Berlin, Secr. TIB1-B7, Gustav-Meyer-Allee 25,  
D - 13355 BERLIN, Germany  
Email : [savidis@tu-berlin.de](mailto:savidis@tu-berlin.de)

<sup>2</sup> Ditto.  
Email: [daniel.aubram@tu-berlin.de](mailto:daniel.aubram@tu-berlin.de)

<sup>3</sup> Ditto.  
Email: [frank.rackwitz@tu-berlin.de](mailto:frank.rackwitz@tu-berlin.de)

<sup>4</sup> Ditto.  
Email: [winfried.schepers@tu-berlin.de](mailto:winfried.schepers@tu-berlin.de)

Because of the dependency of sand on the stress state, density state and drainage conditions as well as on the loading history, the continuum mechanical approach is rather complicated. Only a few of recent contributions simulate the mechanical behaviour of sand over a wide range of densities and stress states using a single set of parameters, whereas classical soil models treat the diverse appearances as different materials. Furthermore, the specific characteristics of granular media render the problem highly non-linear and, therefore, can only be solved numerically. It turns out that the choice of the computational tool is as important as the mathematical modelling of the material.

The remaining paper is structured as follows. In section 2, the elastoplastic CSSA-Model [Li, 2002] is presented as example of advanced constitutive modelling. Based on the numerical implementation of the model into a finite element code, section 3 shows results of the simulation of monotonic and cyclic element tests. The capabilities of the constitutive equation are used in section 4 to simulate the shear wave propagation due to harmonic and seismic excitation. The paper closes with some concluding remarks in section 5.

## 2. THE CSSA-MODEL

To account for the above mentioned facts of sand behavior, the critical state sand model (CSSA-Model) [Li, 2002] incorporates a state dependent dilatancy, which is defined as the ratio of volumetric and deviatoric strains. There are three concepts in the history of material modelling which affected the development of the elastoplastic CSSA-Model. The well known Critical State framework [Roscoe and Schofield and Wroth, 1958] is effectively the basic idea. To model the response of sand under cyclic loading, the Bounding Surface Plasticity concept [Dafalias, 1986] has been implemented. The Generalized Plasticity framework [Pastor and Zienkiewicz and Chan, 1990] circumvents the difficulty to formulate the hardening and softening functions precisely by describing only the rate of these functions, also referred to as the plastic moduli.

Consider three specimen of the same sand with the same loading history and starting from the same stress state, but with different densities. If a shear loading increment from the same stress ratio  $\eta = p'/q$  is applied, the loose sand tends to contract and the dense sand tends to dilate, like shown in the triaxial  $p'$ - $q$ -plane in Figure 1, where  $p' = (\sigma'_1 + 2\sigma'_3)/3$  and  $q = \sigma'_1 - \sigma'_3$ .  $\sigma'_1$  and  $\sigma'_3$  are the axial and the radial effective stress, respectively. In addition, medium-dense and dense sand passes a so-called phase transformation state [Ishihara and Tatsuoka and Yasuda, 1975], [Li and Dafalias, 2000]. At this point the dilatancy  $D$  is equal to zero, although the sand is not at a critical state.

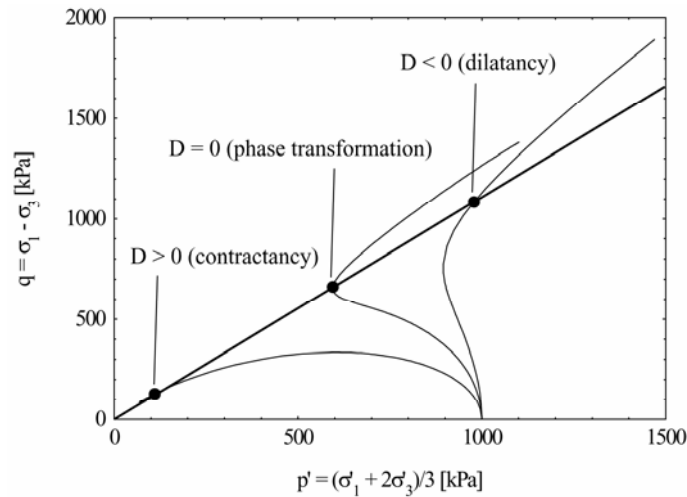


**Figure 1: Undrained response of sand with different densities under the same confining pressure**

Li [Li, 1998] has shown that there exists a linear representation of the critical state line (CSL) in the  $e-(p'/p_a)^\xi$ -plane, where  $e$  is the void ratio,  $p_a$  is the atmospheric pressure at sea level and  $\xi$  is a material parameter (Figure 2). The internal state parameter  $\psi$  can be defined from Figure 2 as

$$\psi = e - e_c = e - \left[ e_\Gamma - \lambda_c \left( p'/p_a \right)^\xi \right], \quad (1)$$

where  $e_\Gamma$  and  $\lambda_c$  are material parameters.

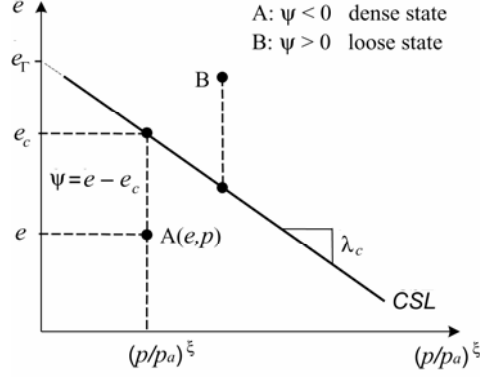


**Figure 2: Critical state line (CSL) and state parameter  $\psi$ .**

One of the main features of the CSSA-Model is the state dependent dilatancy, due to the fact that the dilatancy for sand depends on the stress ratio as well as on the void ratio. The dilatancy function  $D_1$  for the first bounding surface (Figure 3) has the form

$$D_1 = \frac{d_1}{M_c g(\theta)} \left[ M_c g(\theta) e^{m\psi} \sqrt{\frac{\rho_1^*}{\rho_1}} - R \right], \quad (2)$$

where  $d_1$ ,  $M_c$ ,  $m$  are material parameters. The CSSA-Model includes 15 material parameters determined from drained and undrained triaxial tests.  $\rho_1$ ,  $\rho_1^*$  are the mapping distances referred to the Bounding Surface Plasticity framework. The function  $g(\theta)$ , where  $\theta$  is the Lode angle, establishes the shape of the first bounding surface and  $R$  is an invariant of the stress ratio tensor  $r_{ij} = s_{ij}/p'$ , where  $s_{ij}$  is the deviatoric stress tensor.

The CSSA-Model defines two bounding surfaces,  $F_1$  and  $F_2$ , which are shown in Figure 3. Bounding surface  $F_1$  forms a cone around the hydrostatic axis ( $\sigma_1 = \sigma_2 = \sigma_3$ ) restricted by a flat cap which represents the second bounding surface  $F_2$ . The current stress state is always located on a loading surface.

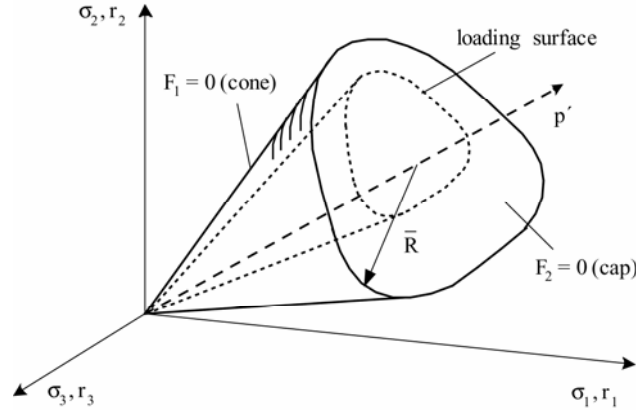


**Figure 3: Bounding surfaces and loading surfaces of the CSSA-Model.**

### 3. NUMERICAL IMPLEMENTATION

Because most of the geotechnical problems can only be solved numerically, a numerical representation of the soil model is needed. In a finite element code, the iteration of the global equilibrium is often done by a Newton-Raphson iteration scheme (Figure 4). The local stress update, also referred to as the stress point algorithm, can be derived by an Euler method.

There are two groups of stress point algorithms. The explicit stress point algorithms are formulations using well known terms at the beginning of an increment, like the forward Euler scheme. Implicit stress point algorithms are formulations using terms at the end of an increment, like the backward Euler scheme. As a matter of fact,

implicit algorithms usually require a specific formulation of the yield surface. Therefore, the application to generalized plasticity models, especially to the CSSA-Model, needs further investigations. The CSSA-Model has been implemented into the general purpose finite element code ANSYS using the material model interface “usermat” [Rackwitz, 2003], [ANSYS Inc., 2000].

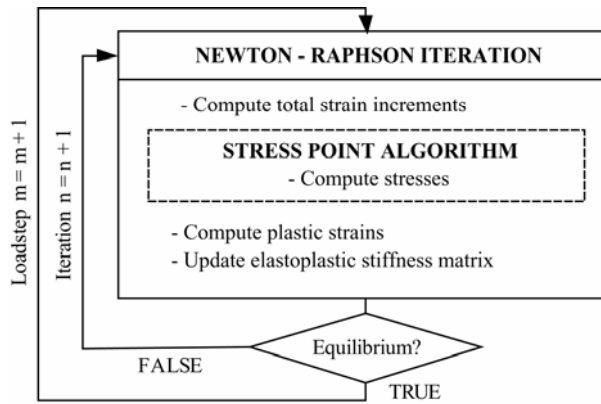
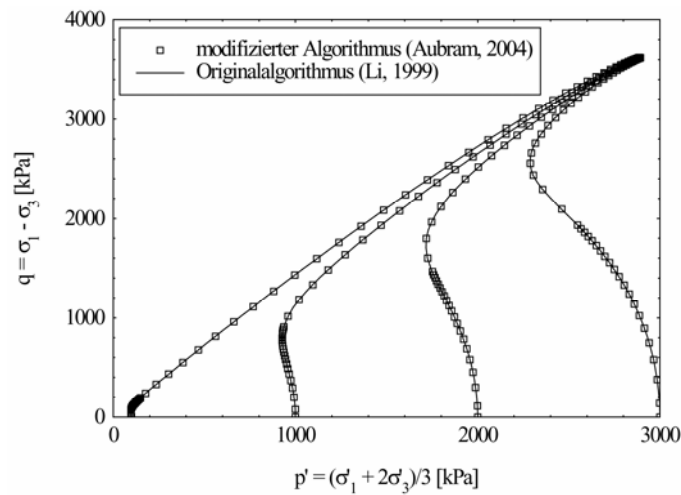
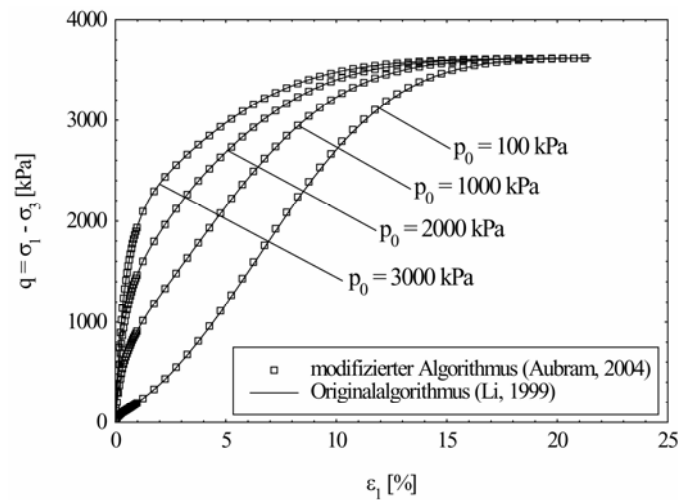


Figure 4: Flowchart of the Newton-Raphson iteration of the global equilibrium.



(a)



(b)

Figure 5: Simulation of undrained triaxial compression tests, Toyoura sand,  $D_r = 65\%$ .

The implementation of the CSSA-Model in ANSYS has been tested by simulation of element tests [Rackwitz, 2003], [Aubram, 2004]. In particular, the validation focuses on drained and undrained triaxial compression tests, undrained cyclic triaxial tests and cyclic oedometer tests. For the following numerical simulation of element tests the material parameters for Toyoura sand [Li, 2002] have been used. Figure 5 shows the simulation of an undrained triaxial compression test with Toyoura sand and four different initial confining pressures in the  $p'$ - $q$ -plane (Figure 5a) and  $\varepsilon_1$ - $q$ -plane (Figure 5b), where  $\varepsilon_1$  is the axial strain.

The solid line show the results of the original stress point algorithm [Li, 1999]. In this integration scheme, the size of the strain increments given by the global equilibrium iteration remains unchanged and the stress increment results from an iteration. The circle marks denote an alternative explicit algorithm [Aubram, 2004], in which the coarse strain increments are divided into a number of substeps defined by the user. However, the results of both algorithms coincide in this simulation. Simulations of the experimental results of monotonic triaxial tests using the CSSA-Model are quite well, which has been presented by [Li and Dafalias, 2000].

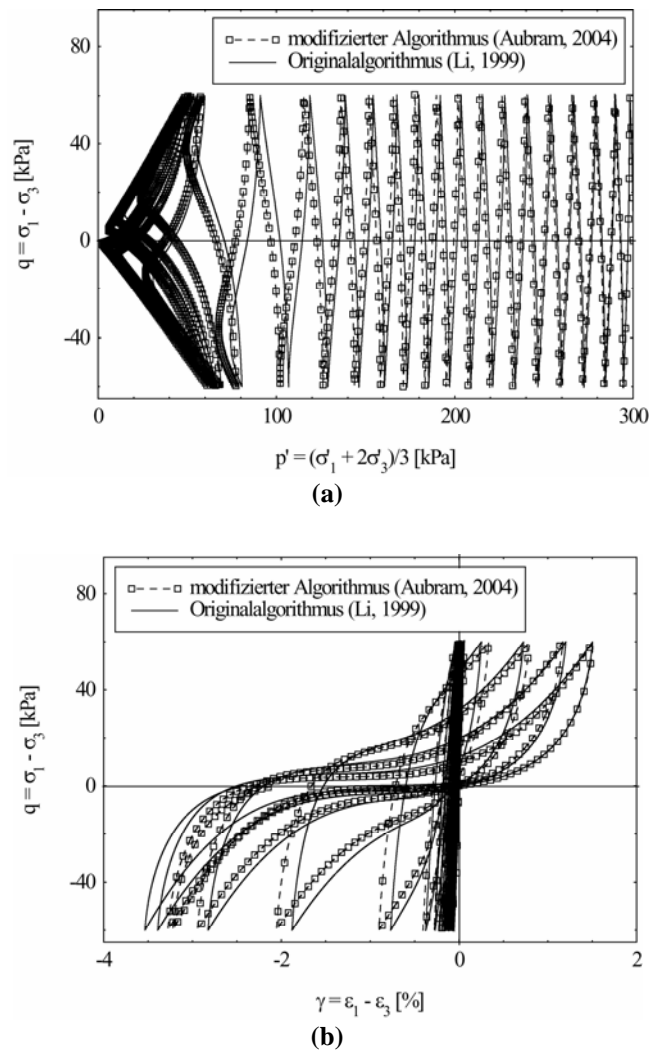


**Figure 6: Simulation of a cyclic undrained triaxial test, Toyoura sand,  $D_r = 65\%$ .**

In contrast to that, the results of the simulation of a cyclic undrained triaxial test differ slightly, dependent on the size of the integration increments, as shown in the  $p'$ - $q$ -plane (Figure 6a) and  $\varepsilon_1$ - $q$ -plane (Figure 6b). Since the explicit substepping algorithm is only exact if the increments are infinite small, the calculation error accumulates along with the number of load steps. Notwithstanding this fact, the CSSA-Model again provides good results. If the number of loading cycles increases, starting from isotropic consolidation, the effective mean normal stress decreases at constant density as a result of a rearrangement of the particles. In the vicinity of  $p' = 0$  kPa, the sand shows cyclic mobility, staying within the bounding surfaces.

Focussing on bounding surface  $F_2$  on the hydrostatic axis, the CSSA-Model also formulates the response of sand under oedometric conditions, as shown in Figure 7. Although the current model version captures the cyclic

behaviour under these conditions only rudimentarily, the CSSA-Model simulates the hysteresises under repeated loading and unloading quite well.

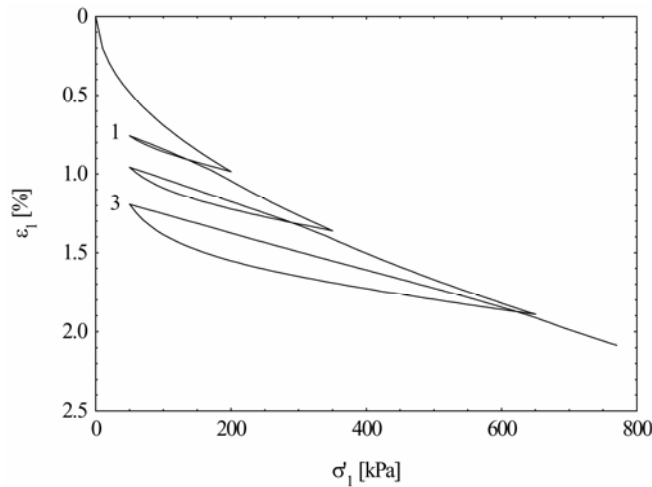


**Figure 7: Simulation of an cyclic oedometer test, Toyoura sand,  $D_r = 65\%$ .**

#### 4. APPLICATION TO SHEAR WAVE PROPAGATION

The goal arising from the preceding sections is the numerical simulation of the shear wave propagation in a sand layer, resulting from an earthquake excitation of a rigid half space at the base of the deposit. As a first approximation, if the excitation is parallel to the boundaries this can be modelled as a one-dimensional problem, involving a single shear component [Seed and Idriss, 1970]. When applying the finite element method it turns out that pure, i.e. bending-free shearing can not be handled by the majority of one-dimensional finite elements. However, plane distorted quadrilateral elements in combination with vertical and horizontal coupling of nodes of the same row can be applied instead. Undrained conditions are adopted by disabling the vertical displacements of the top nodes. Figure 8 shows the ground profile and the finite element mesh used for the subsequent analysis.

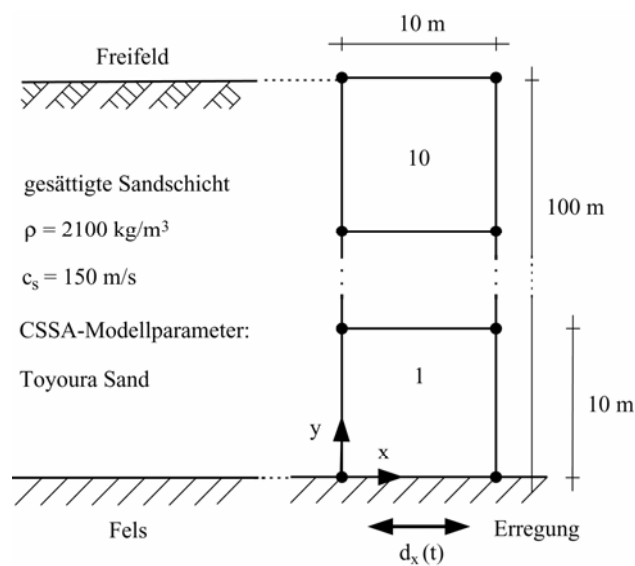


**Figure 8: Ground profile and finite element mesh used for the simulation of shear wave propagation.**

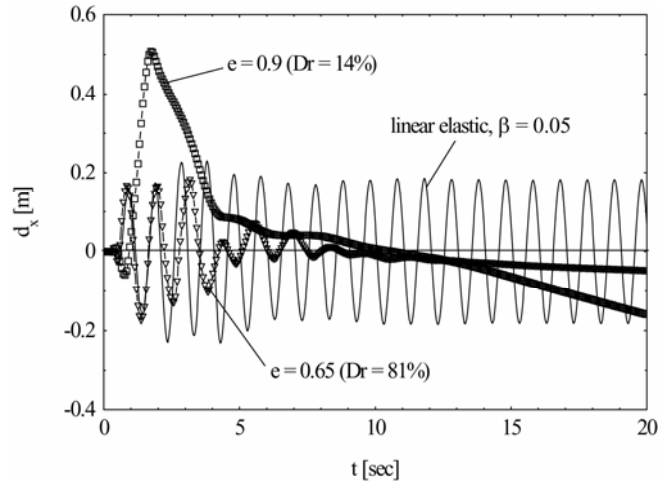


**Figure 9: Horizontal displacements on ground surface under harmonic excitation and undrained conditions.  $f = 1$  Hz,  $d_{x,max} = 0.1$  m, Toyoura sand.**

Firstly, the base was excited with  $f = 1$  Hz and  $d_{x,max} = 0.1$  m harmonically in order to test the FE-model and the behaviour of the constitutive equation under undrained conditions. Three types of soil were observed: a linear elastic material with damping ( $\beta = 0.05$ ), Toyoura sand in a loose state ( $D_r = 14\%$ ) and Toyoura sand in a medium to dense state ( $D_r = 81\%$ ). After the first cycle the loose sand undergoes large displacements and then resets after a few seconds, as shown in the time history of the ground surface response in figure 9. It seems that the upper regions of the loose soil deposit “creep” along with the excitation without any cyclic shape.

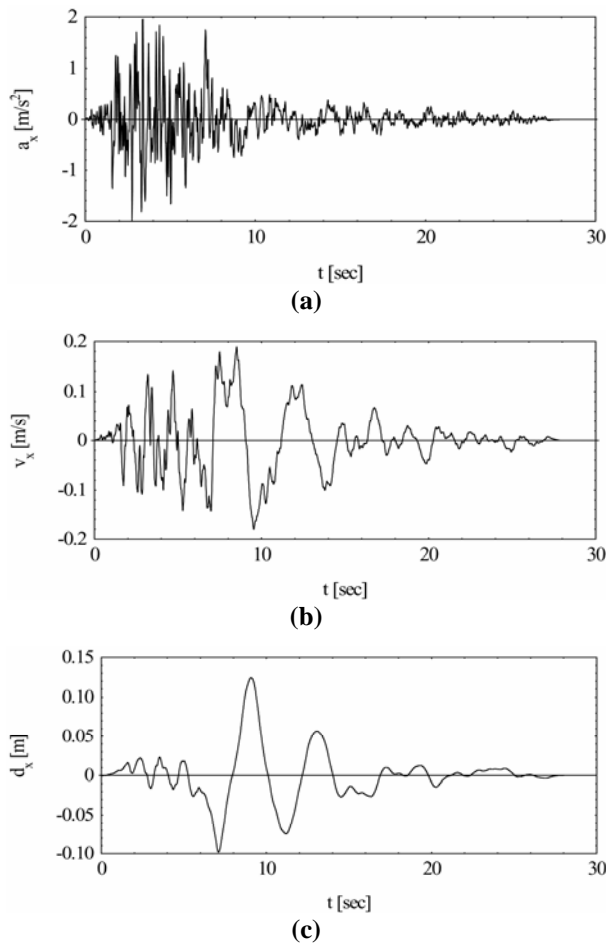


**Figure 10: Baseline corrected signal of the San Fernando earthquake, 02/09/1971, 2:00 pm, HP = 0.2 Hz, LP = 35 Hz. (a) Acceleration time history, (b) velocity time history, (c) displacement time history.**

For the simulation of the shear wave propagation under seismic loading, the well known San Fernando earthquake from February 2, 1971 has been applied to the base of the deposit. The acceleration time history was registered in Hollywood, Los Angeles lateral to the direction of propagation from the source. When using ANSYS or other FE-codes for dynamic calculations, it is often convenient to input a time-displacement curve rather than acceleration data, due to the degrees of freedom of the finite elements. To this end, figure 10 shows the baseline corrected acceleration, velocity and displacement of the signal with a high pass of  $HP = 0.2$  Hz and a low pass of  $LP = 35$  Hz. Based on the FE-model shown in figure 8, one gets the results after a few minutes of computation time.

Since a full set of the material parameters of the CSSA-model is not available for soils found in the area of Los Angeles, the parameters for Toyoura sand [Li, 2002] are borrowed. This, of course, limits quantitative precise results but not the phenomenological representation of sand. Again, two different densities are observed: loose sand with  $D_r = 14$  % and medium to dense sand with  $D_r = 81$  %. Figure 11a and 11b present the undrained response of the sand layer in 25 m depth in the  $p'$ - $\sigma_{xy}$ -plane. It can be seen that the decrease of  $p'$  in the case of the medium to dense sand is limited, whereas it vanishes in the case of the loose sand. The effective mean normal stress of the loose sand drops very quickly, whereas the medium to dense sand shows cyclic mobility response. It seems that the higher amplitude of the shear stress compensates the decrease of the normal effective stresses.

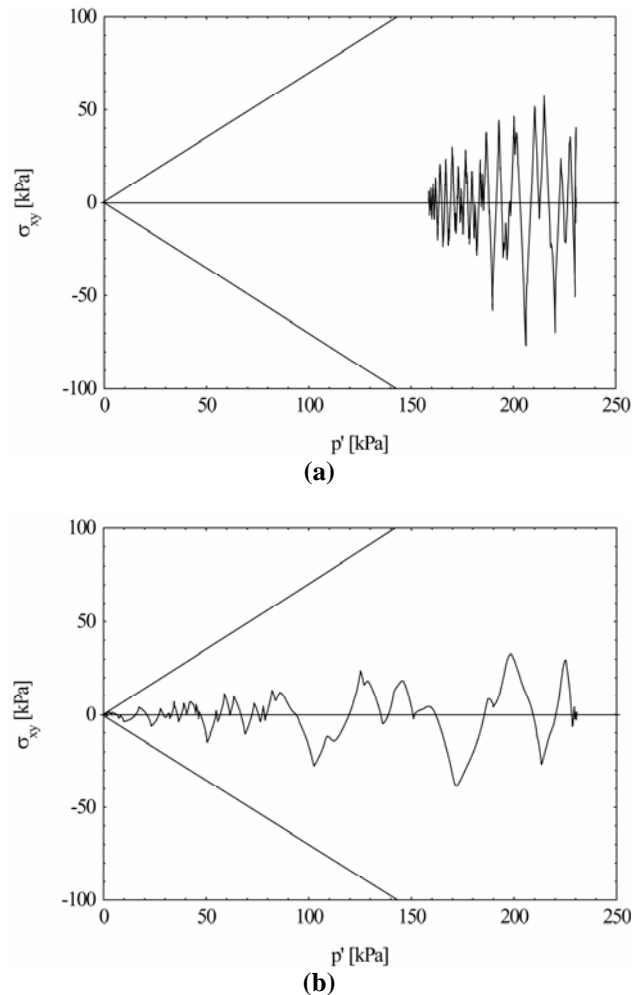
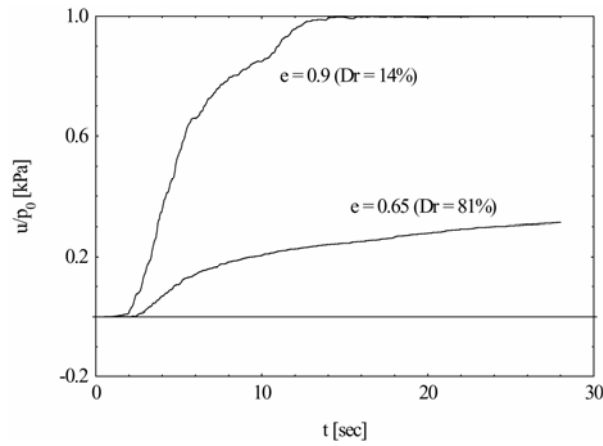


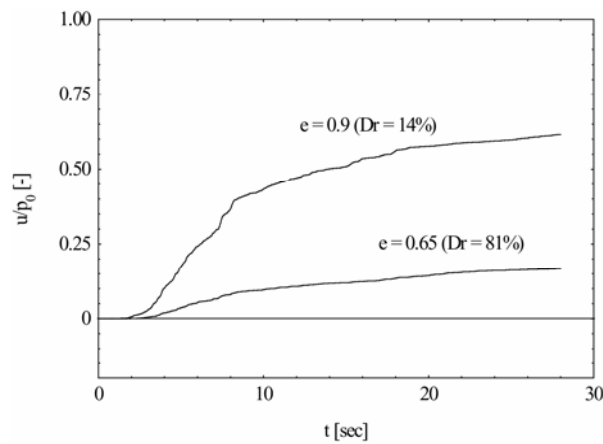
**Figure 11: Stress path in  $p'$ - $s_{xy}$ -plane at 25 m depth under seismic excitation and undrained conditions. San Fernando earthquake, Toyoura sand. (a)  $e_0 = 0.65$  ( $D_{r0} = 81$  %), (b)  $e_0 = 0.90$  ( $D_{r0} = 14$  %).**

This behaviour accompanies the excess pore pressure development shown in figure 12a and figure 12b for a depth of 25 m and 50 m, respectively. Irrespective of the depth, the build up of excess pore pressure of the loose sand is considerably larger which would cause large shear deformation. At 25 m depth, the excess pore pressure even matches the initial confining pressure, leading to the liquefaction of this region of the soil layer.





(a)



(b)

**Figure 12: Excessive pore pressure development at different depth under seismic excitation and undrained conditions. San Fernando earthquake, Toyoura sand. (a) At 25 m depth, (b) at 50 m depth.**

## 5. CONCLUSIONS

After an introduction to the advanced constitutive modelling of soils and presenting specific characteristics of granular soils under monotonic and cyclic loading, the elastoplastic CSSA-Model was chosen to model the strong non-linear behaviour under seismic excitation. The model was implemented into the commercial finite element code ANSYS for the subsequent simulation of element test and the analysis of earthquake-induced shear wave propagation in sandy soil deposits. The results show that the constitutive equation is capable to describe the sand behaviour under monotonic and cyclic loading and under drained and undrained conditions over a wide range of densities and stress states with only one set of material parameters. Moreover, the CSSA-Model, due to its concept of state dependent dilatancy, also models the different response of loose and dense sand under seismic loading quite realistically. The constitutive equation captures density developments and vertical displacements of the ground surface under drained conditions, which has not presented here. Under undrained conditions, a pore pressure build up in the soil profile may occur, followed by a decrease of the effective stresses. Thus, conclusions can be drawn about the cyclic mobility of the sand deposit or the exposure to liquefaction. Finally, these results point out the capabilities of advanced constitutive equations for soils in earthquake engineering.

Nevertheless, the numerical simulation of element tests show that the stress point algorithm and the size of the calculation increments play a crucial role in the application of elastoplastic models and have to be further investigated. It seems reasonable to implement other stress point algorithms, especially implicit algorithms in further investigations and to adjust the formulation of the plastic moduli to enhance the model response to arbitrary boundary value problems.

## 6. REFERENCES

- ANSYS Inc. (2000), *Guide to ANSYS 5.6 User Programmable Features*
- Aubram, D. (2004), Implementierung eines geeigneten 'Stress Point Algorithm' in das Li-Stoffgesetz in ANSYS, Diploma Thesis, *Soil Mechanics and Foundation Engineering Division, Technical University of Berlin* [in German]
- Dafalias, Y.F. (1986), Bounding Surface Plasticity I: Mathematical Foundation and Hypoplasticity, *Journal of Engineering Mechanics*, Vol. 112, No. 9, pp. 966-987
- Ishihara, K., Tatsuoka, F. and Yasuda, S. (1975), Undrained Deformation and Liquefaction of Sand under Cyclic Stresses, *Soils and Foundations*, Vol. 15, No. 1, pp. 29-44
- Li, X.S. (1998), Linear Representation of Steady-State Line, *Journal of Geotechnical and Geoenvironmental Engineering*, Vol. 124, No. 12, pp. 1215-1217
- Li, X.S. (1999), *Implementation of CSSA-Model into the FE-Code SUMDES*, Personal Communication
- Li, X.S. (2002), A Sand Model with State Dependent Dilatancy, *Géotechnique*, Vol. 52, No. 3, pp. 173-186
- Li, X.S. and Dafalias, Y.F. (2000), Dilatancy for Cohesionless Soils, *Géotechnique*, Vol. 50, No. 4, pp. 449-460
- Pastor, M., Zienkiewicz, O.C. and Chan, A.H.C. (1990), Generalized Plasticity and the Modelling of Soil Behaviour, *International Journal for Numerical and Analytical Methods in Geomechanics*, Vol. 14, pp. 151-190
- Rackwitz, F. (2003), Numerische Untersuchungen zum Tragverhalten von Zugpfählen und Zugpfahlgruppen in Sand auf der Grundlage von Probelastungen, PhD Thesis, *Soil Mechanics and Foundation Engineering Division Series, No. 32, Technical University of Berlin*, S.A. Savidis (ed.) [in German]
- Roscoe, K.H., Schofield, A.N. and Wroth, C.P. (1958), A Sand Model with State Dependent Dilatancy, *Géotechnique*, Vol. 8, No. 1, pp. 22-53
- Seed, H.B. and Idriss, I.M. (1970), Soil Moduli and Damping Factors for Dynamic Response Analysis, *Earthquake Engineering Research Center, University of California*, Report No. UCB/EERC 70-10